STRUCTURAL
BIOLOGY

Volume 72 (2016)

Supporting information for article:

Transmission electron microscopy for the evaluation and optimization of crystal growth

Hilary P. Stevenson, Guowu Lin, Christopher O. Barnes, Ieva Sutkeviciute, Troy Krzysiak, Simon C. Weiss, Shelley Reynolds, Ying Wu, Veeranagu Nagarajan, Alexander M. Makhov, Robert Lawrence, Emily Lamm, Lisa Clark, Timothy J Gardella, Brenda G. Hogue, Craig M. Ogata, Jinwoo Ahn, Angela M. Gronenborn, James F. Conway, Jean-Pierre Vilardaga, Aina E. Cohen and Guillermo Calero

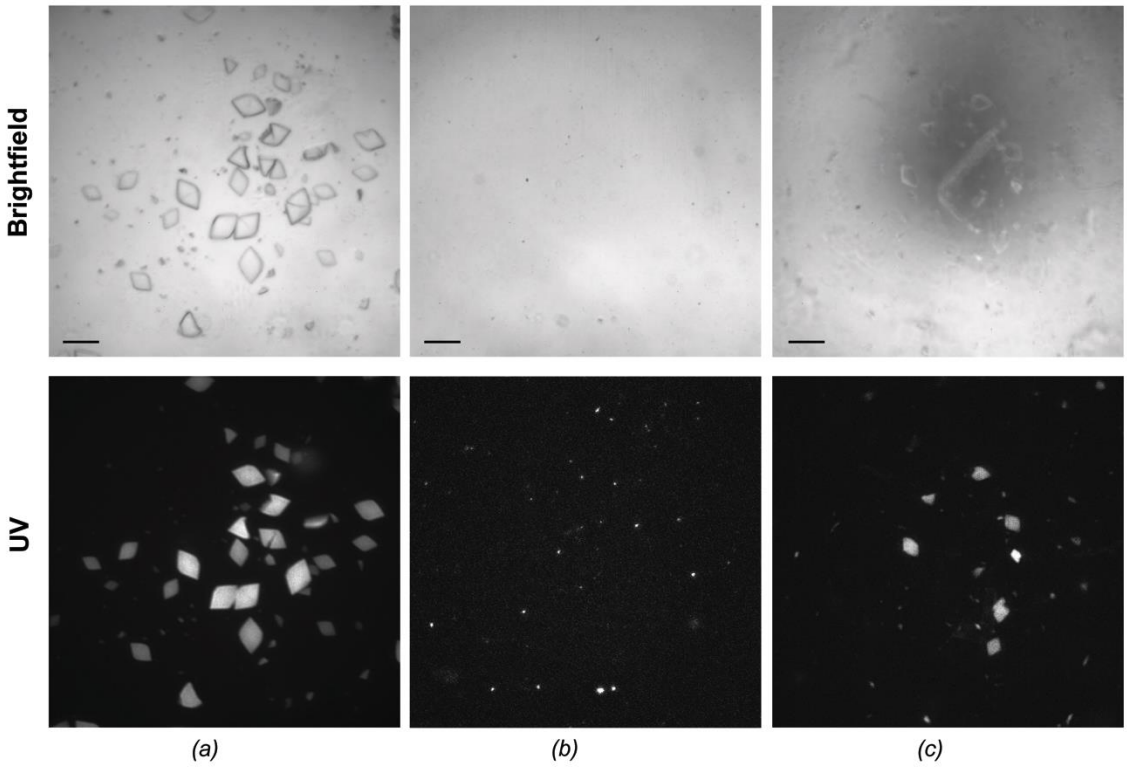

Figure S1 UV and brightfield images of wild type Pol II nanocrystals before and after crushing with beads. (a) Intact crystals used for fragmentation experiments. (b) Crystals fragmented using 0.5 mm beads (see main text section 2.2) which resulted in homogeneously sized fragments measuring less than 5 μm in size. (c) Crystal fragments resulting from use of a single 3 mm Teflon bead according to the manufacture's protocol (Hampton). Fragments were 2-5 times larger than in (b). (Scale bars: 100 μM). (See main Fig. 1.)

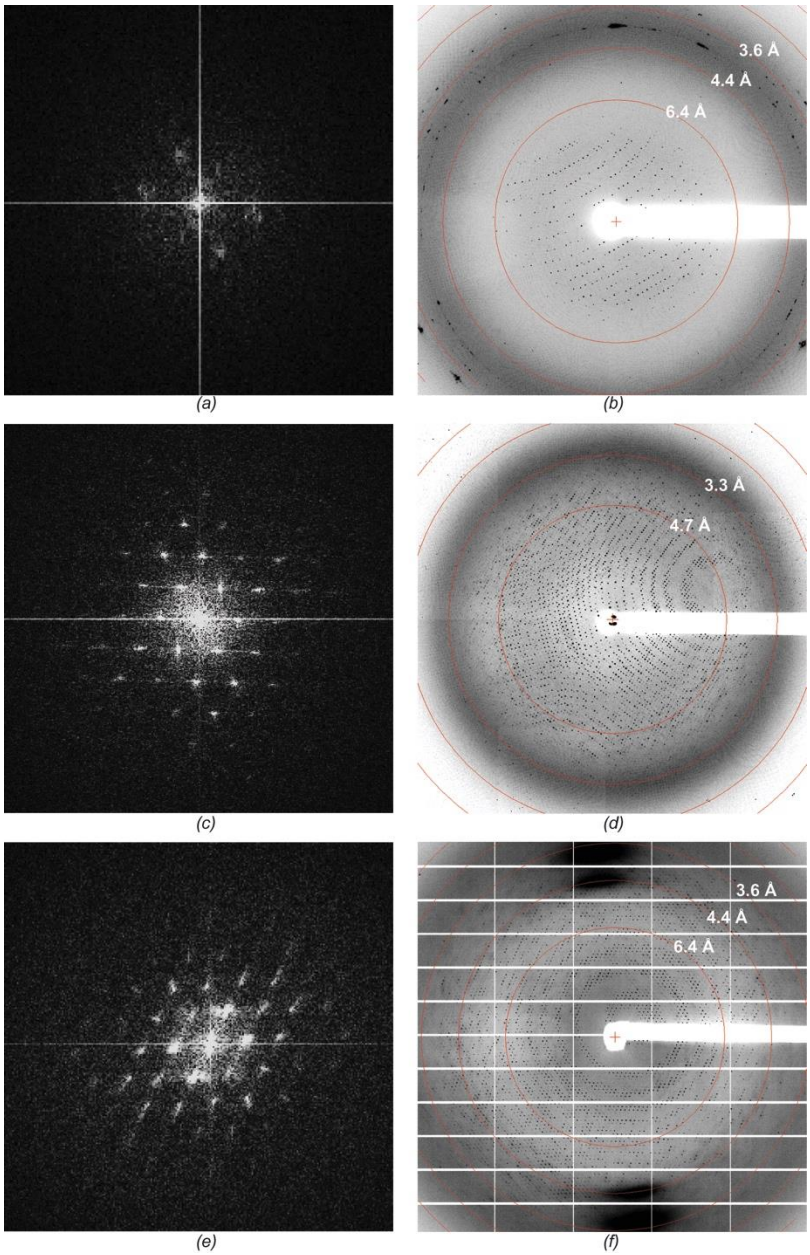

Figure S2 Correlating Fourier analysis of TEM images with synchrotron diffraction images. Fourier transforms of lattices (left panels) positively correlate with diffraction images observed at synchrotron sources (right panels), with higher order Bragg spots being a good indicator of higher resolution diffraction. (a,b) Rtf1 (c,d) *E. coli* dGTPase, post-dehydration protocols (see experimental), (e,f) wild-type RNA Polymerase II. (see main Fig. 2.)

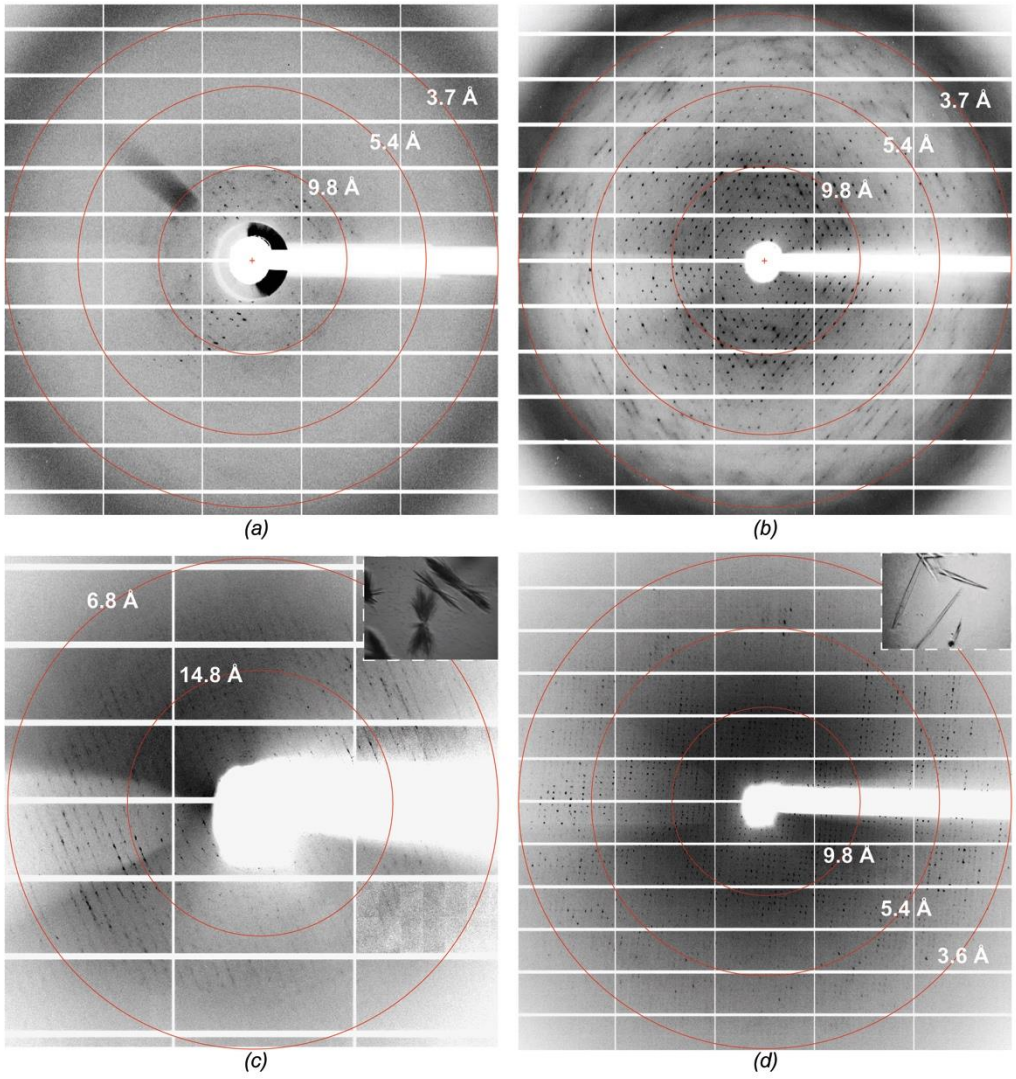

Figure S3 Optimizing X-ray diffraction. (a) For UNG2-Vpr-DCAF1-DDB1 crystals, characteristic diffraction images of crystals in similar cryo-conditions as previously published structures revealed poor diffraction to ~9 Å. After TEM revealed lattices (see Fig. 2) showed high-ordered Bragg spots, (b) changes in cryo-protectant resulted in improved diffraction to ~3.7 Å. (c) Similarly, DCAF1-DDB1 crystal clusters (inset) diffracted to ~6 Å, but upon the addition of additives (d) single crystal (inset) diffraction improved to beyond 3.6 Å. As seen in Fig. 2, the presence of well-ordered lattices for these crystals also suggested improvements in crystallization could result in improved diffraction. (See main Fig. 2.)

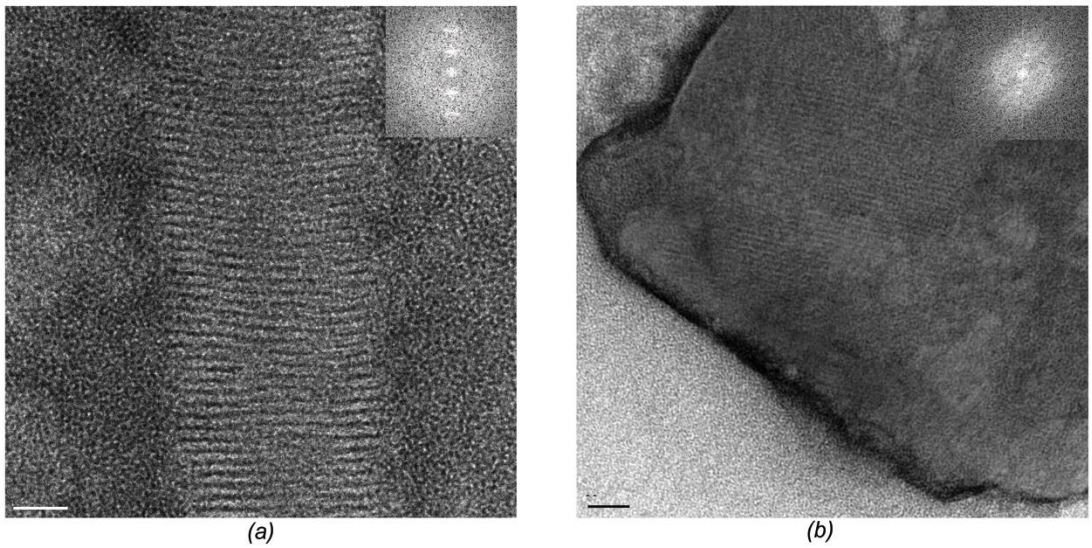

Figure S4 TEM analysis of parathyroid hormone receptor (PTHR) crystals. (a) Wild-type PTHR1 and (b) Bril-PTHR1 show poor quality lattices. Large crystals of this target have not been reported, but fragmentation of granular aggregates from crystallography experiments showed nanoseed lattices that could be detected by TEM. These crystals however may be a starting material for matrix-microseeding. (Scale bars: 50 nm). (See main Fig. 2.)

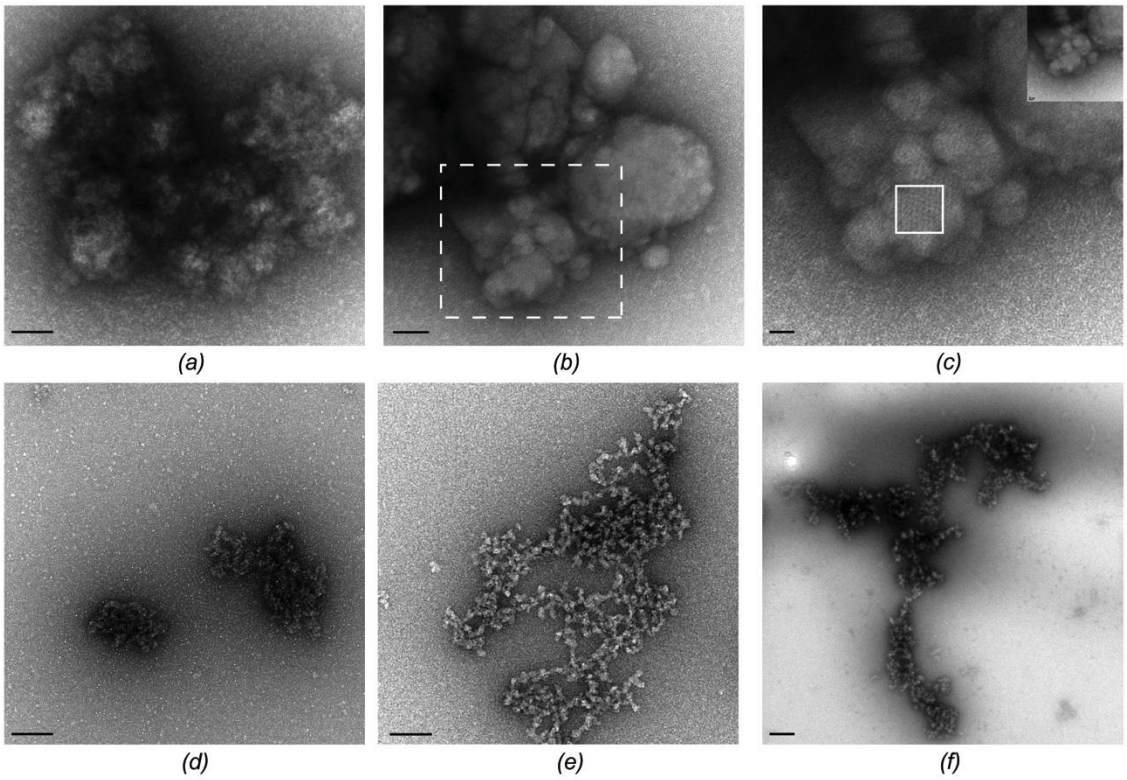

Figure S5 Examples of protein aggregates common amongst nanocrystals as visualized by TEM. (a-c) The presence of protein aggregates and nanocrystal nuclei among Globin-X crystals compromise small areas of partially ordered lattices (FFT of boxed area, panel (c)). (d) Pol II-GFP, (e) Wild-type PTHR1 and (f) Bril-PTHR1. (Scale bars: (a) 100 nm; (b) 50 nm; (c) 20 nm; (d-f) 50 nm). (See main Fig. 2.)

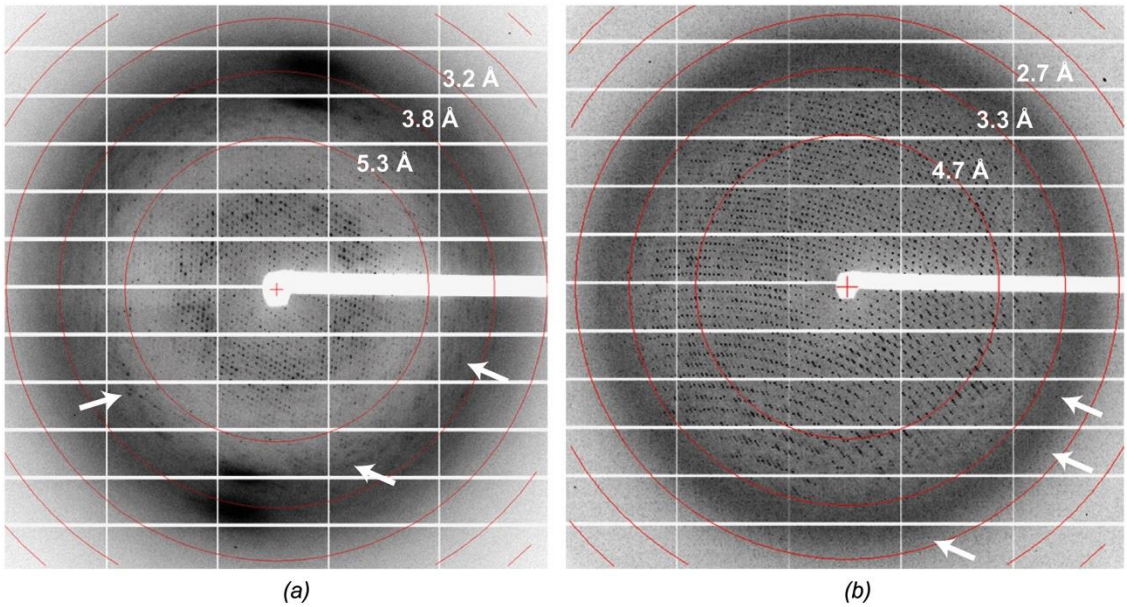

Figure S6 dGTPase dehydration diffraction comparison. Characteristic diffraction images of dGTPase crystals pre- (a) and post- (b) dehydration protocols. Arrows represent maximum observed reflections of ~ 4.3 and 2.9 Å, respectively. (See main Fig. 7.)

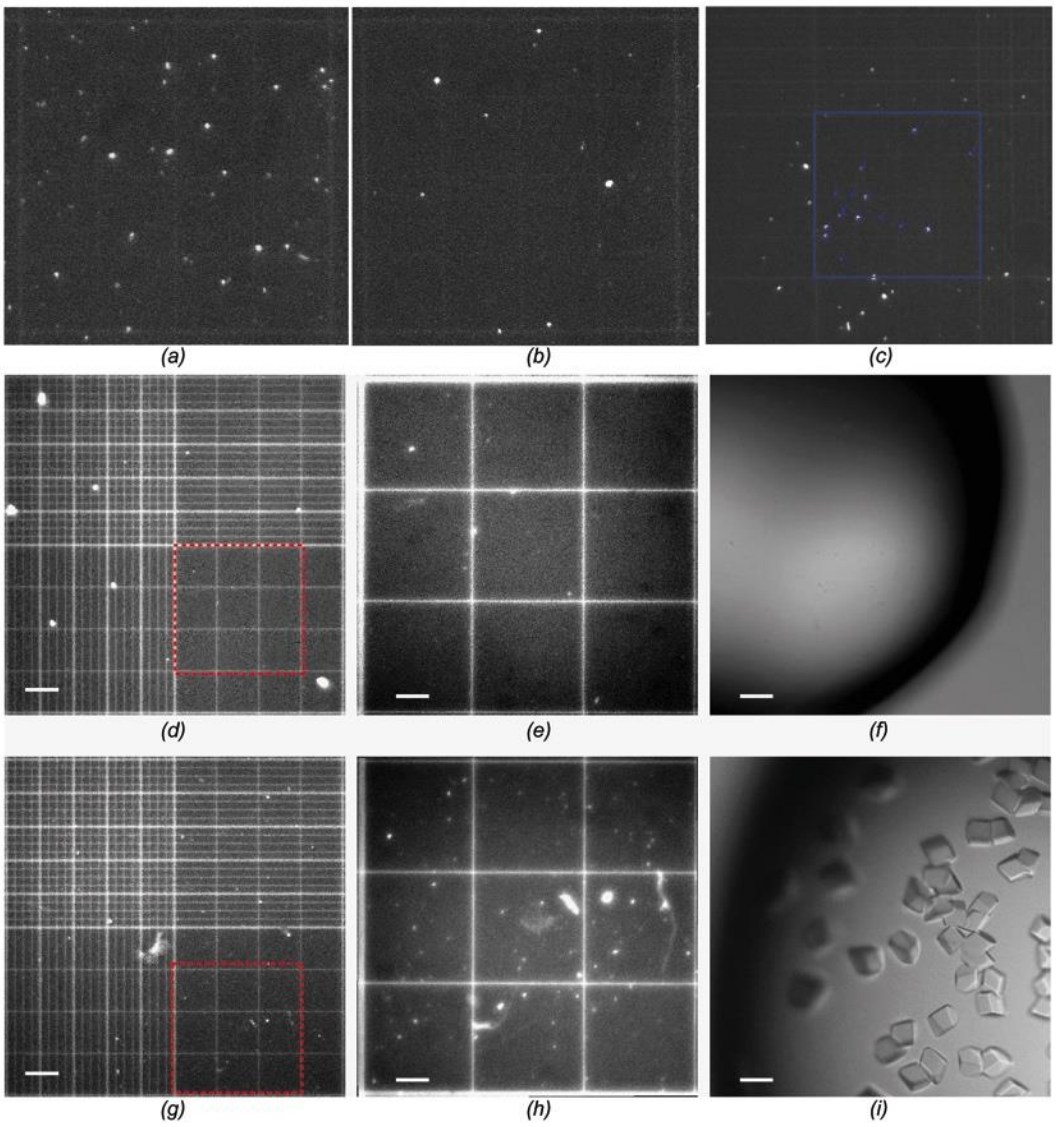

Figure S7 UV tryptophan fluorescence image of seed concentration determination using a haemocytometer. Seeds were counted by pipetting them into the counting chamber of the haemocytometer, covering with a thin UV transparent coverslip, taking a UV fluoresce microscopy image and counting visualized seeds using ImageJ software (see main text section 2.4). (a) Undiluted seeds, (b) 1:4 dilution of seeds. Total seed counts calculated for the 1x stock taken from (a) and (b) were on average of 330 seeds per µL. (c) Lower magnification (5x) image of haemocytometer with seeds showing the ImageJ counting overlay. In addition, crystals were fragmented with either 0.1 mm (d-f) or 0.5 mm (g-i) beads and quantified with a haemocytometer. Nominal 15x zoomed images revealed significantly higher detectable concentrations of seeds from 0.5 mm bead fragmentation (h) versus 0.1 mm beads (e). Seeding experiments show that over a one week duration, seeds generated from 0.1 mm beads (f) show no

crystals while 0.5 mm bead fragments (i) grew large crystals (Scale bars: (a,b) 200 μm; (c,d) D 75 μm; (e,f) 100 μm). (See main Fig. 9.)

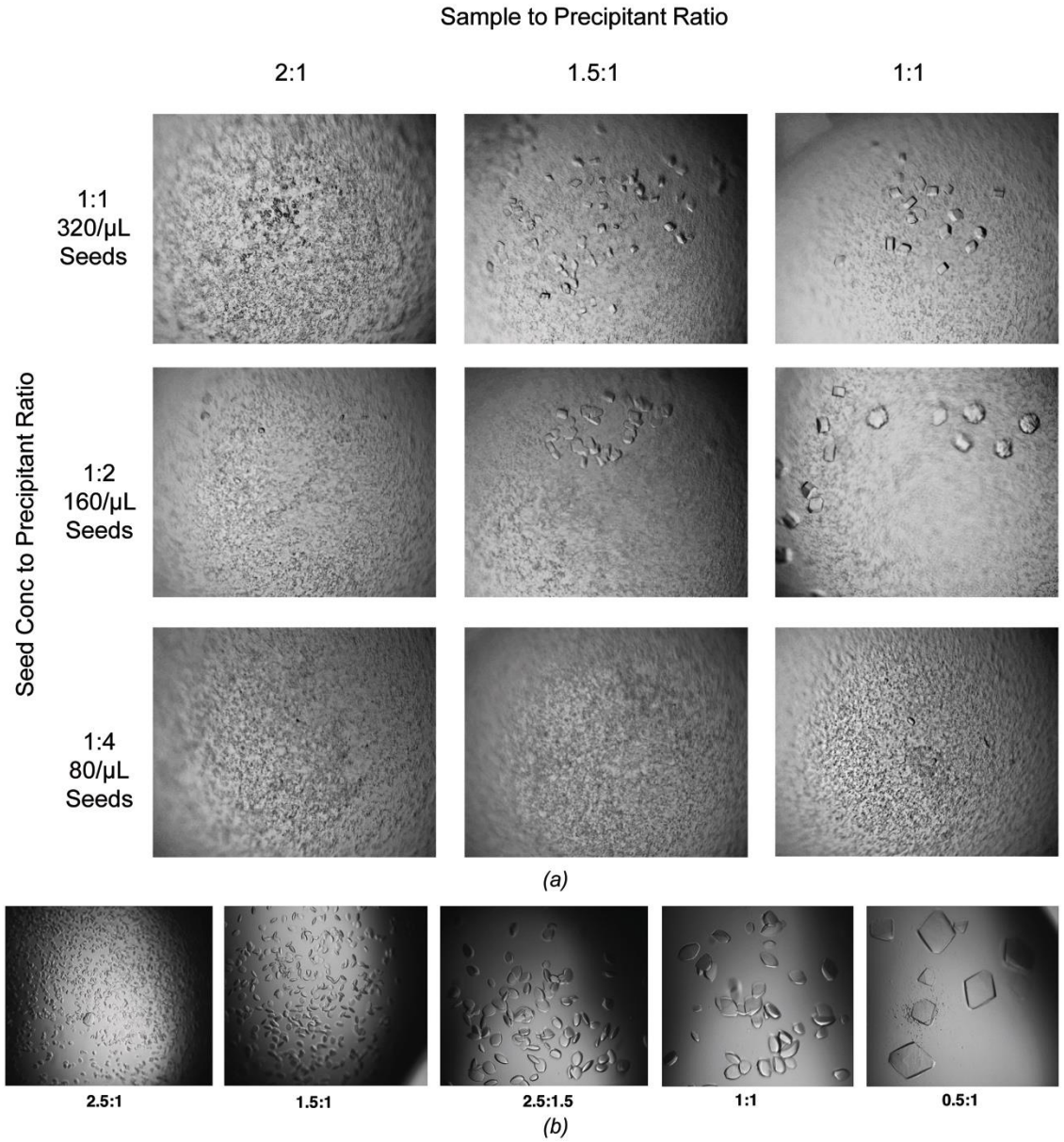

Figure S8 Generating crystal catalogues. Fragmented crystals were prepared using 0.5 mm beads as described in main text section 2.2 (a) Comparison of the effect of varying the precipitant to sample ratio with the effect of quantified seed concentration. (b) Refinement of crystal sizes was performed by varying the precipitant to protein ratio. In all cases the same amount crystalline slurry was added to the crystallization drop. (See main Fig. 9.)